Supporting Information

Dense Platinum Nanoparticles Confined in Mn-N-C Nanocages for Robust Heavy-Duty PEMFCs

Lei Zhao[#,a,b], Zhenmin Cao[#,c], Jiayu Zuo[a], Mingliang Yang[b], Hongyan Qiao[c], Jun Song Chen[a] and Rui Wu[a,*]

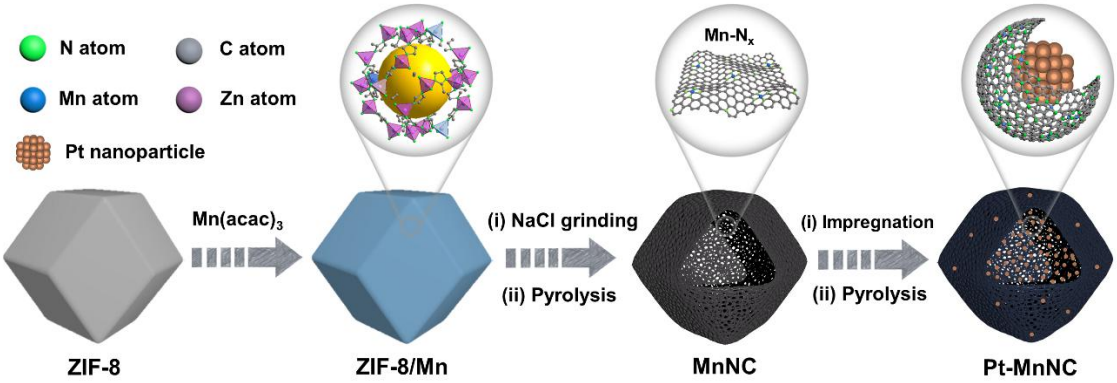

Fig. S1. Schematic diagram of the synthetic procedure for Pt-MnNC.

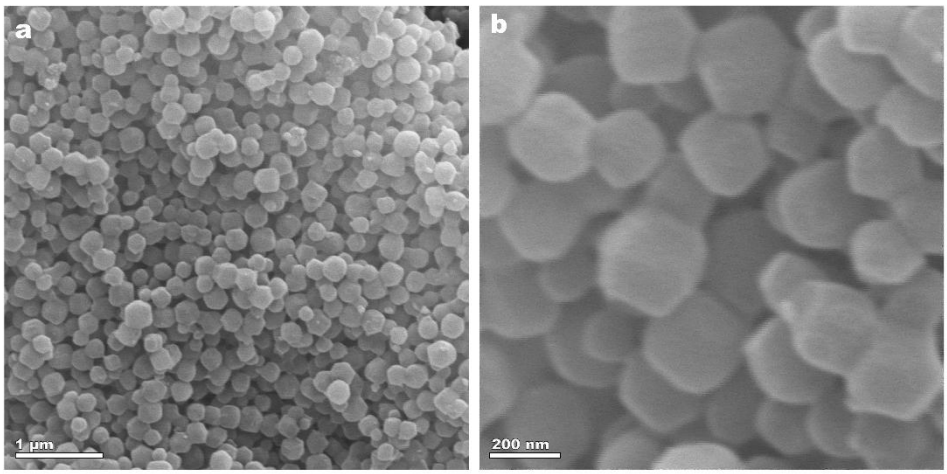

Fig. S2. (a, b) SEM images of ZIF-8.

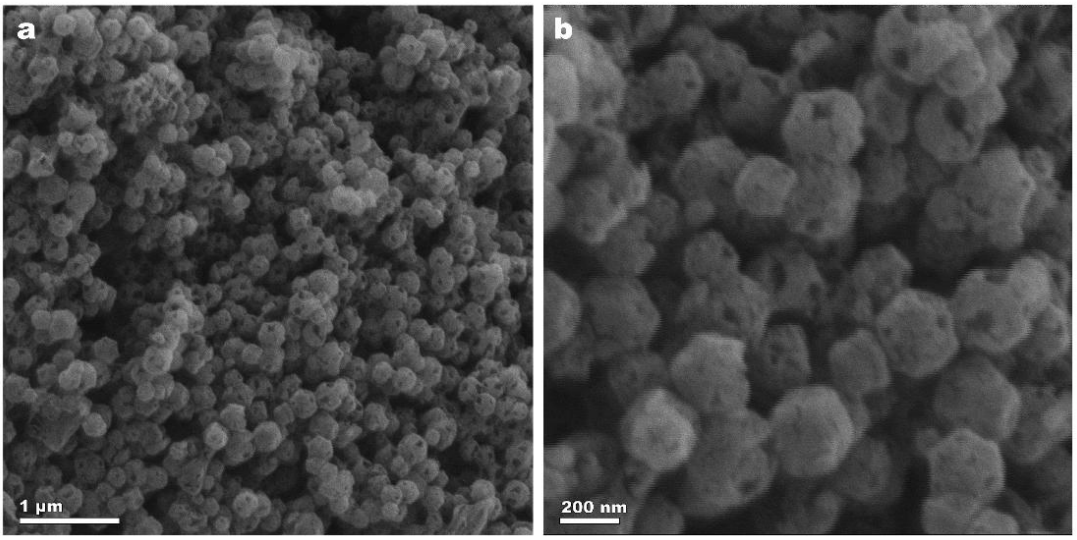

Fig. S3. (a, b) SEM images of MnNC.

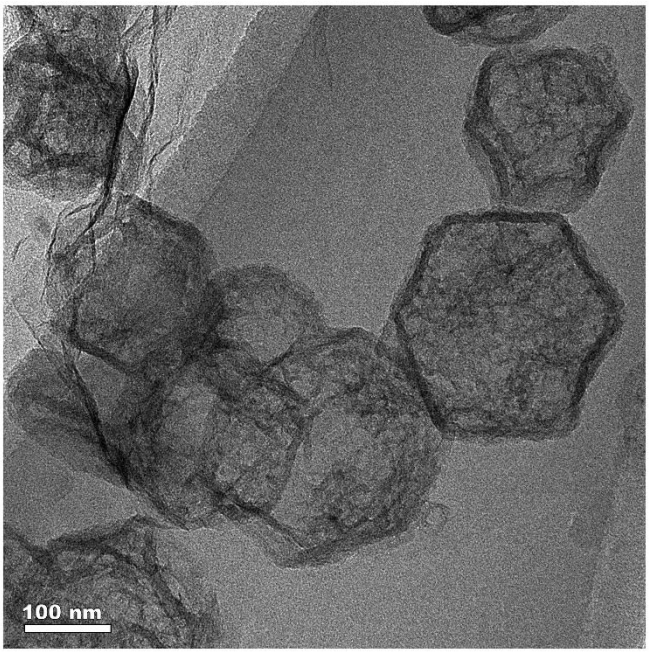

Fig. S4. TEM image of MnNC.

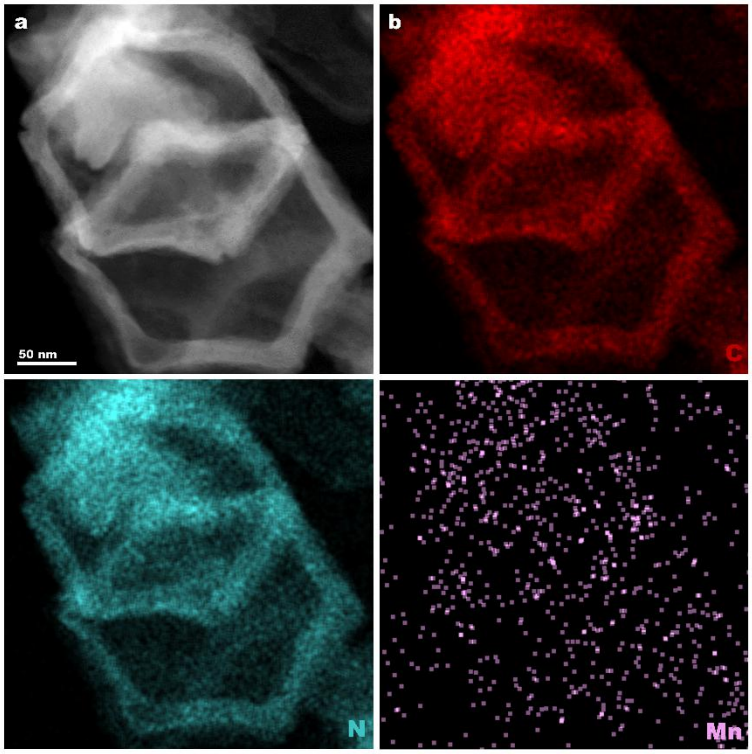

Fig. S5. HAADF-STEM image and corresponding EDS elemental mappings of MnNC.

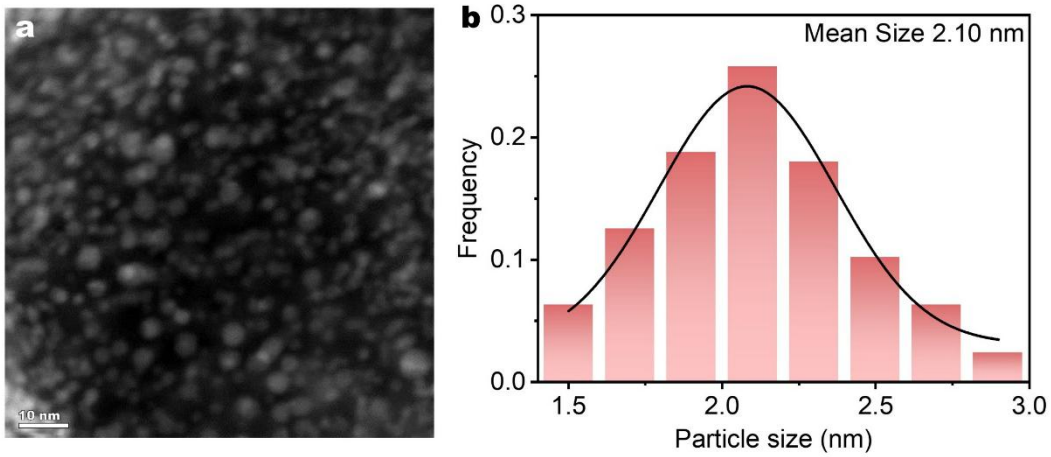

Fig. S6. (a) HAADF-STEM image and (b) corresponding particle size distributions histogram of Pt-MnNC.

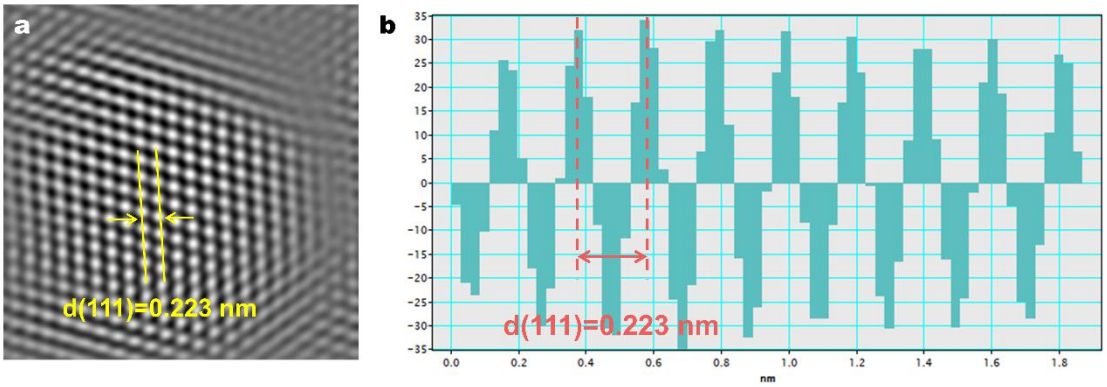

Fig. S7. (a) Fast Fourier transform HR-TEM image and (b) intensity profiles of obtained from (a) of Pt-MnNC.

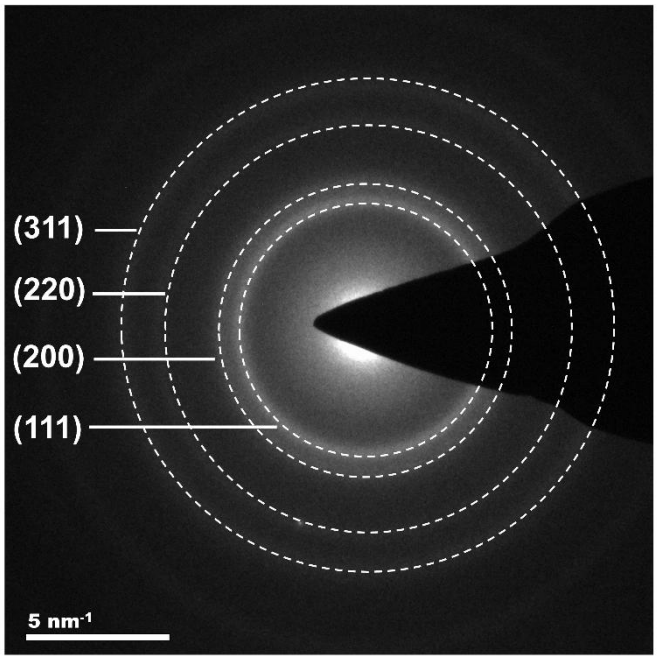

Fig. S8. SAED image of Pt-MnNC.

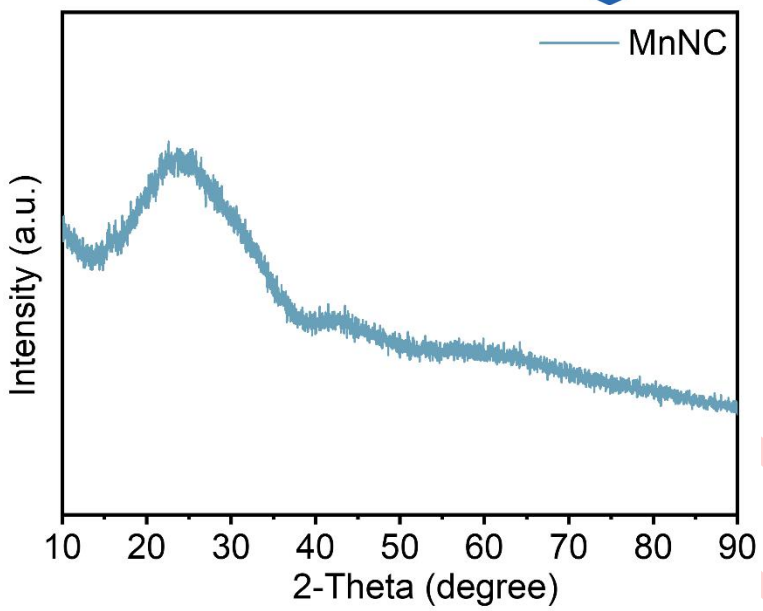

Fig. S9. XRD spectra of MnNC.

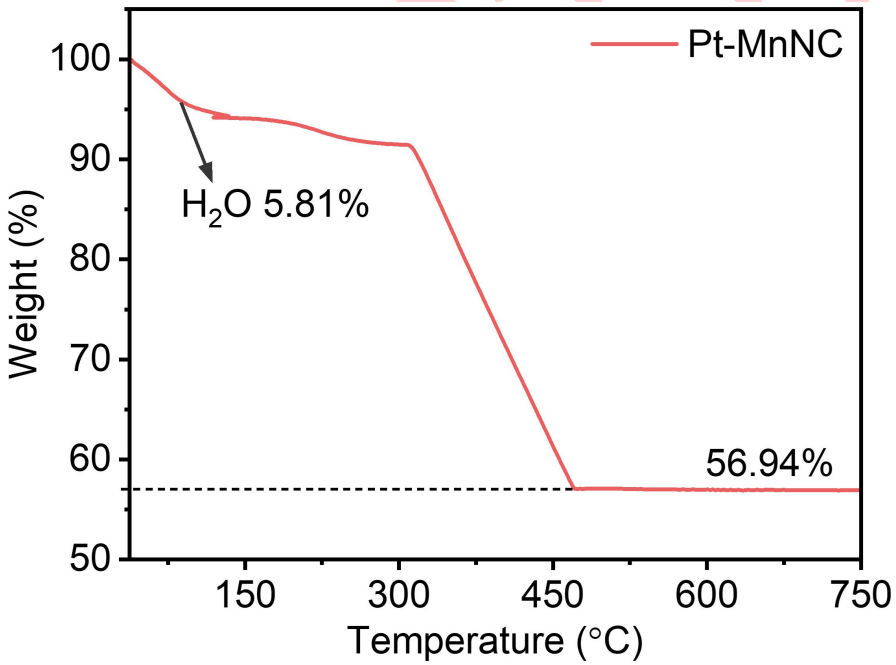

Fig. S10. TGA curve of Pt-MnNC.

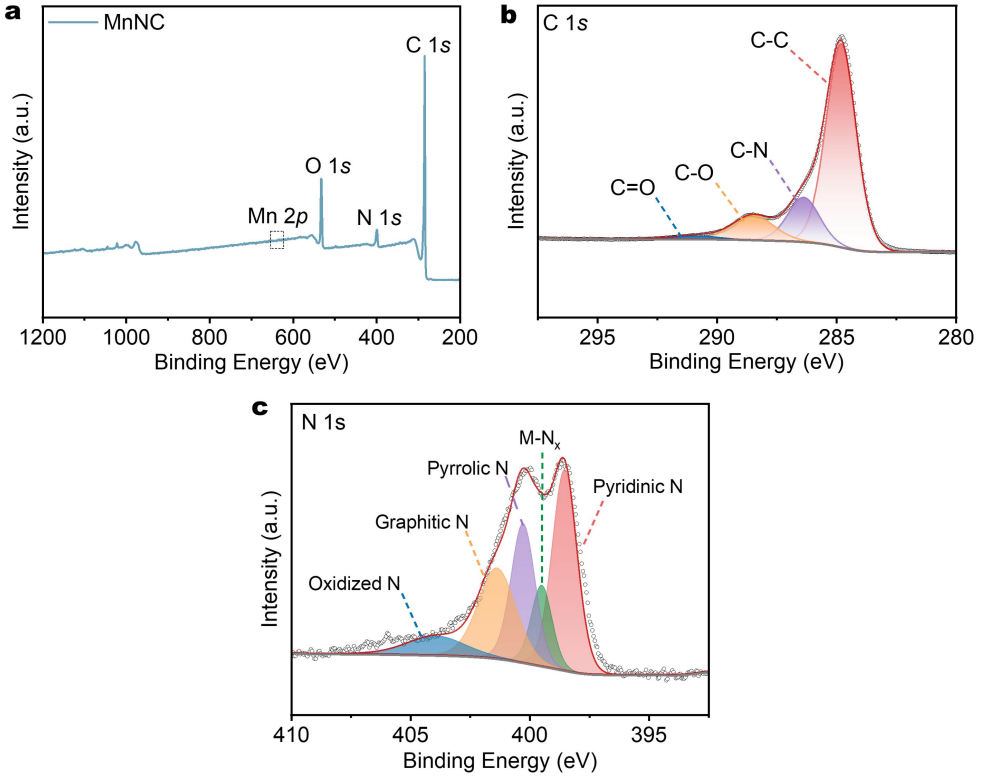

Fig. S11. XPS survey spectra of (a) MnNC and corresponding high-resolution (b) C 1*s* spectrum (c) N 1*s* spectrum.

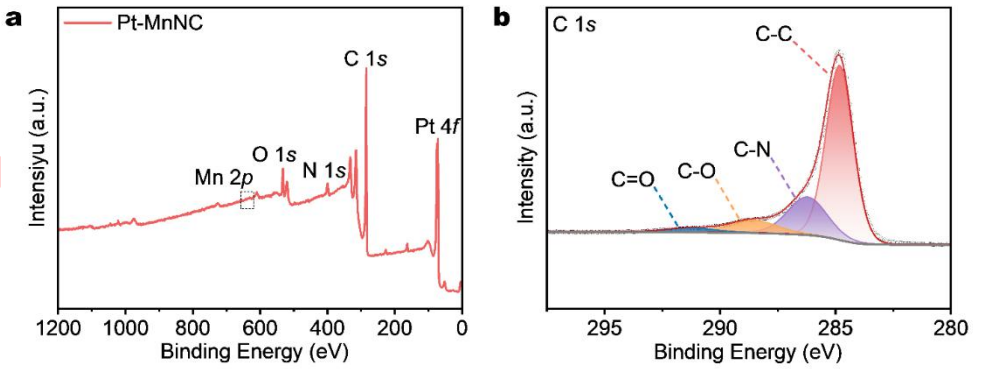

Fig. S12. XPS survey spectra of (a) Pt-MnNC and corresponding high-resolution (b) C 1s spectrum.

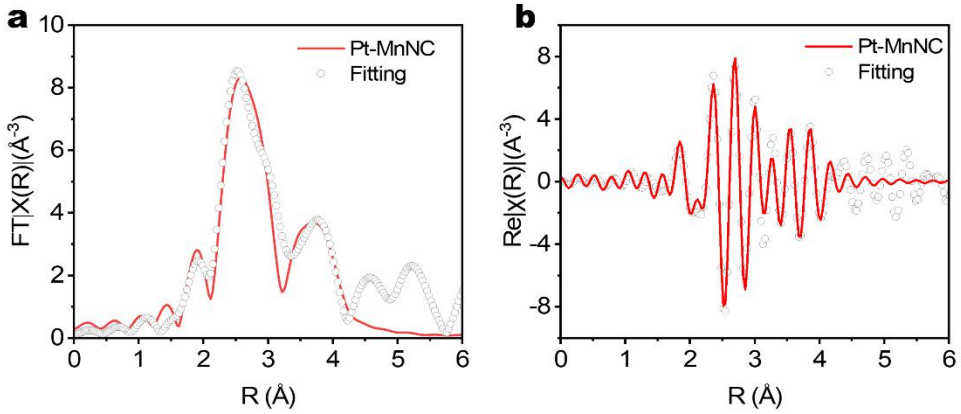

Fig. S13. EXAFS fitting result of (a) Pt L_3-edge and (b) corresponding k space for Pt-MnNC.

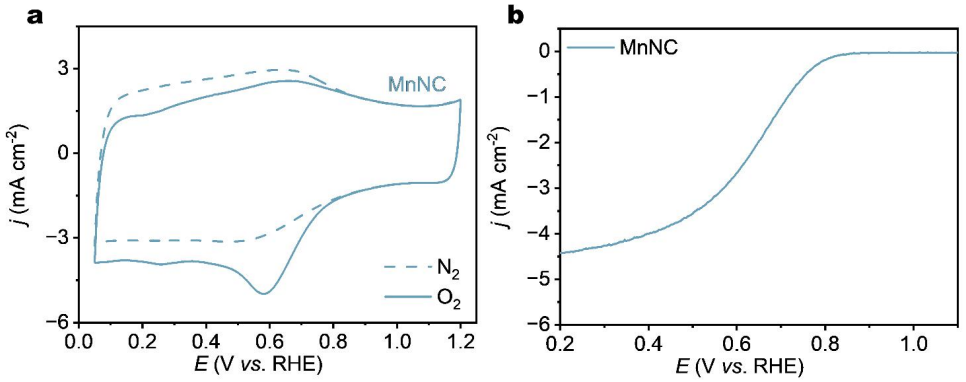

Fig. S14. The electrochemical performance of MnNC. (a) CV curves in N_2- and O_2-saturated 0.1 M $HClO_4$ electrolyte at a scan rate of 50 mV s^{-1}. (b) ORR polarization curve at 1,600 rpm with a scan rate of 10 mV s^{-1}.

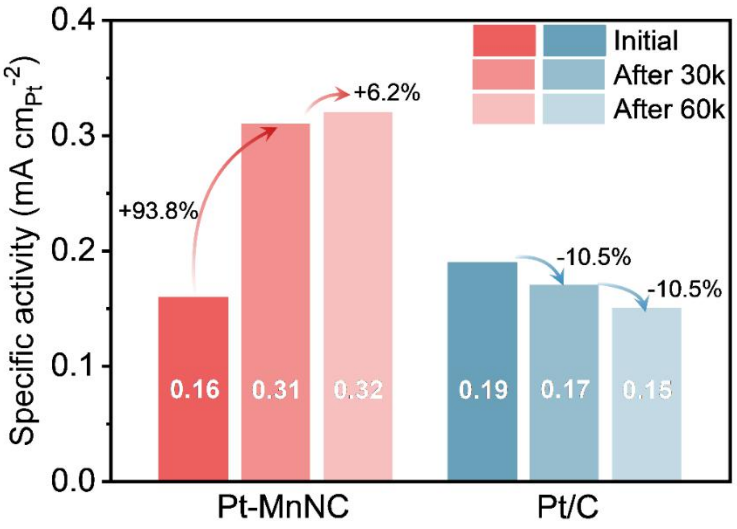

Fig. S15. The evolutions of SA at 0.9 V vs. RHE for Pt-MnNC and Pt/C before and after every 60,000 potential cycles.

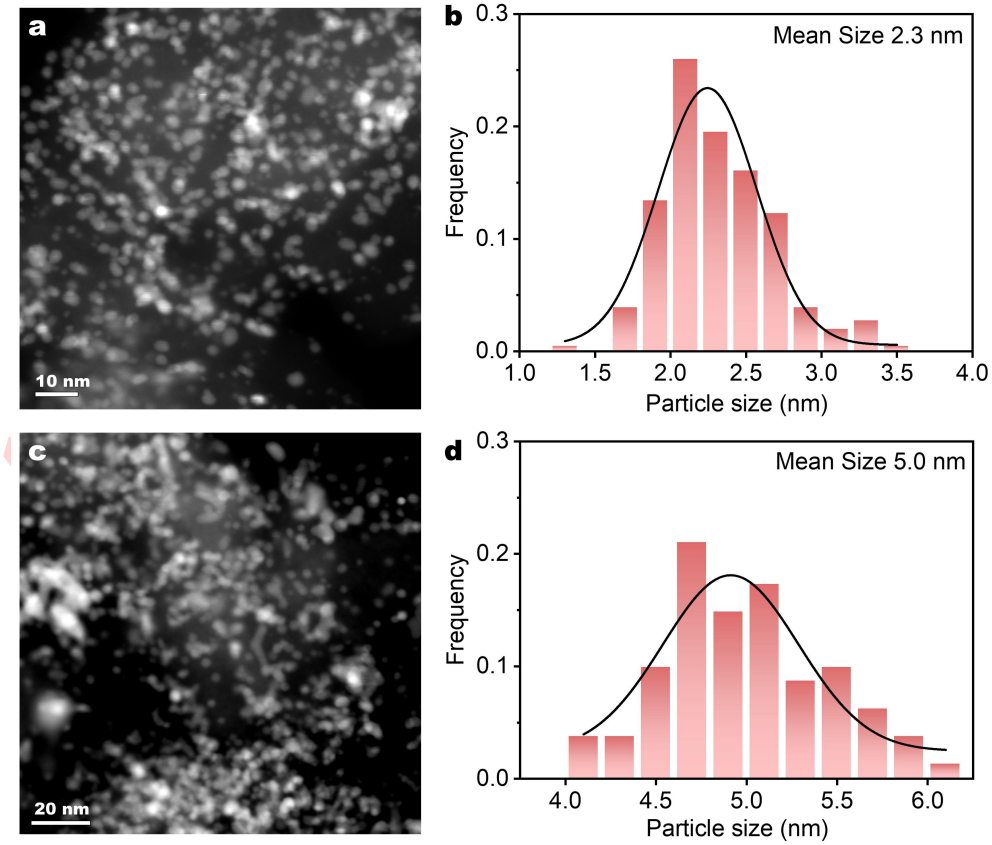

Fig. S16. HAADF-STEM images and corresponding Pt NPs size distributions of (a, b) fresh Pt/C catalyst and (c, d) aged Pt/C catalyst after 60,000 cycles.

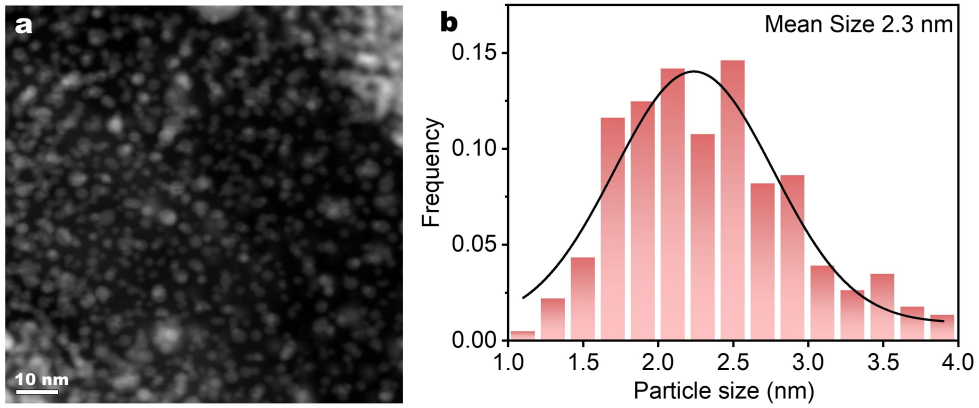

Fig. S17. HAADF-STEM image of (a) Pt-MnNC and (b) corresponding Pt NPs size distributions histogram after 60,000 potential cycles.

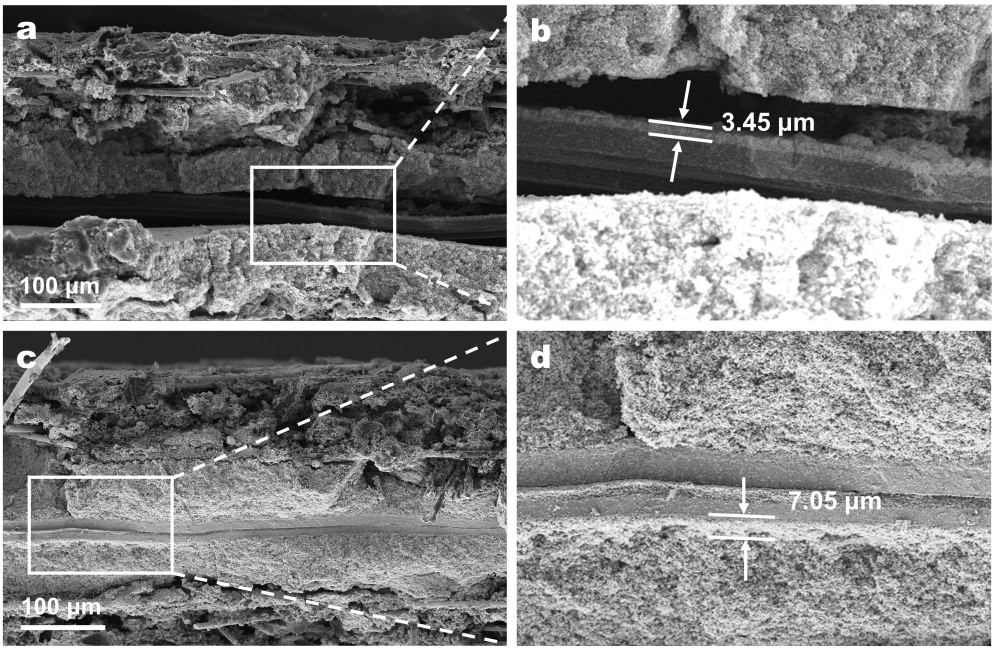

Fig. S18. Cross-sectional SEM images of the cathode catalyst layers with identical Pt loadings of 0.2 mg_{Pt} cm^{-2}. (a, b) Pt-MnNC, (c, d) commercial Pt/C (20 wt%).

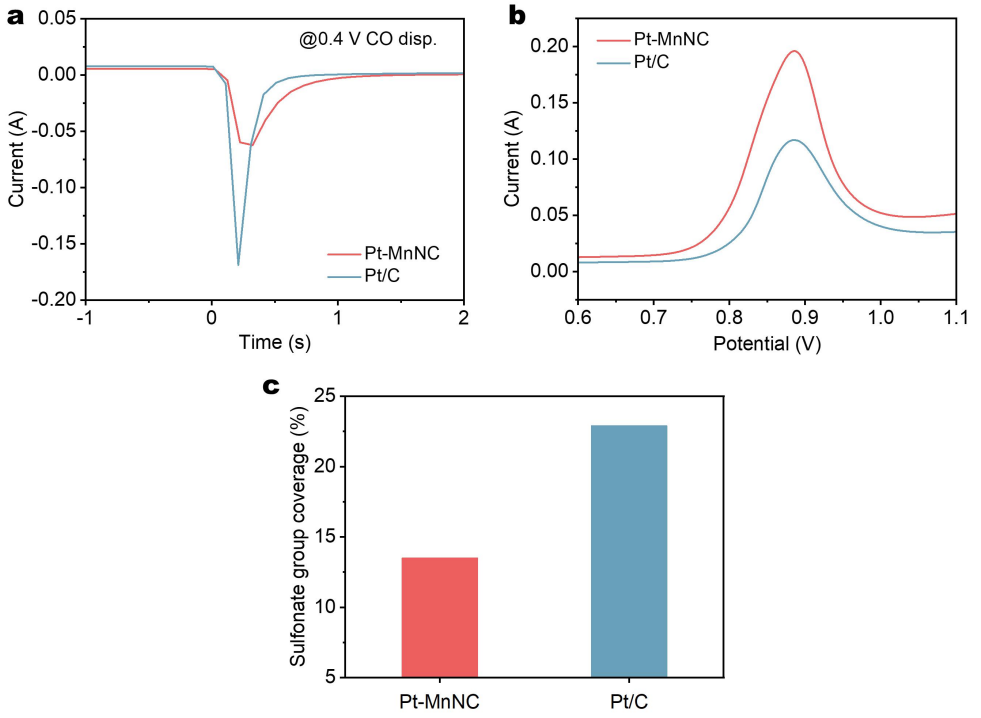

Fig. S19. (a) CO-displacement current density-time curves measured at 0.4 V, (b) CO-stripping curves, and (c) corresponding sulfonate group coverage of Pt-MnNC and commercial Pt/C catalytic layers.

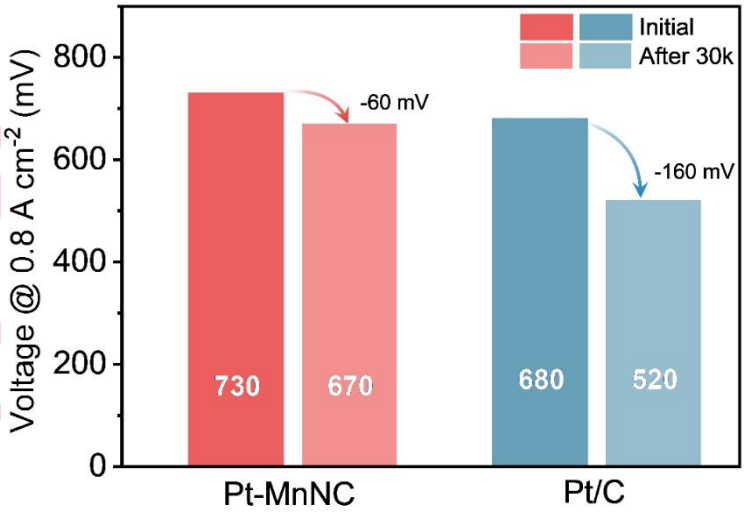

Fig. S20. Cell voltage loss at 0.8 A cm^{-2} after ADT under low-humidity conditions.

Table S1. The Brunauer-Emmett-Teller specific surface area and pore parameters Pt-MnNC and MnNC.

Sample	Pt-MnNC	MnHC
Specific surface area ($m^2\ g^{-1}$)	454.3	1008.8
Average pore radius (nm)	2.13	2.91
Total pore volume ($cm^3\ g^{-1}$)	0.48	1.47

Table S2. Structural parameters extracted from the EXAFS fittings

Sample	Shell	CN[a]	R (Å)[b]	σ^2 ($Å^2 \cdot 10^{-3}$)[c]	ΔE^0 (eV)[d]	R factor (%)
Pt foil	Pt-Pt	12	2.75±0.03	4.2±0.4	7.5±0.5	0.8
Pt-MnNC	Pt-Pt	12	2.81±0.01	4.3±1.6	2.6±3.56	3.8
	Pt-Pt	6	3.92±0.02	1.0±2.0		

CN[a]: coordination number; [b]R: bond distance; [c]σ^2: Debye-Waller factors; [d]ΔE^0: the inner potential correction. R factor: goodness of fit. $S0^2$ was set 0.68, which were obtained from the experimental EXAFS fit of reference Co foil by fixing CN as the known crystallographic value and was fixed to all the samples.